

PAPER • OPEN ACCESS

On the organization and thermal behavior of functional groups on Ti_3C_2 MXene surfaces in vacuum

To cite this article: Ingemar Persson *et al* 2018 *2D Mater.* **5** 015002

View the [article online](#) for updates and enhancements.

You may also like

- [Y-Al_xN thin films](#)
Agn Žukauskaitė, Christopher Tholander, Justinas Palisaitis et al.
- [Comparison between patient-specific deep brain stimulation simulations and commercial system SureTune3](#)
Johannes D Johansson and Peter Zsigmond
- [Cell expansion of human articular chondrocytes on macroporous gelatine scaffolds—impact of microcarrier selection on cell proliferation](#)
Sofia Pettersson, Jonas Wetterö, Pentti Tengvall et al.

OPEN ACCESS

PAPER



RECEIVED

16 May 2017

REVISED

14 August 2017

ACCEPTED FOR PUBLICATION

1 September 2017

PUBLISHED

3 October 2017

Original content from this work may be used under the terms of the [Creative Commons Attribution 3.0 licence](https://creativecommons.org/licenses/by/3.0/).

Any further distribution of this work must maintain attribution to the author(s) and the title of the work, journal citation and DOI.



On the organization and thermal behavior of functional groups on Ti_3C_2 MXene surfaces in vacuum

Ingemar Persson¹, Lars-Åke Näslund¹, Joseph Halim^{1,2}, Michel W Barsoum^{1,2}, Vanya Darakchieva³, Justinas Palisaitis¹, Johanna Rosen¹ and Per O Å Persson¹

¹ Department of Physics Chemistry and Biology, Thin Film Physics Division, Linköpings Universitet, SE-581 83 Linköping, Sweden

² Department of Materials Science and Engineering, Drexel University, Philadelphia, PA 19104, United States of America

³ Department of Physics Chemistry and Biology, Semiconductor Materials Division, Linköpings Universitet, SE-581 83 Linköping, Sweden

E-mail: ingemar.persson@liu.se

Keywords: MXene, $\text{Ti}_3\text{C}_2\text{T}_x$, *in situ* heating, STEM, temperature-programmed XPS, surface functionalization

Supplementary material for this article is available [online](#)

Abstract

The two-dimensional (2D) MXene $\text{Ti}_3\text{C}_2\text{T}_x$ is functionalized by surface groups (T_x) that determine its surface properties for, e.g. electrochemical applications. The coordination and thermal properties of these surface groups has, to date, not been investigated at the atomic level, despite strong variations in the MXene properties that are predicted from different coordinations and from the identity of the functional groups. To alleviate this deficiency, and to characterize the functionalized surfaces of single MXene sheets, the present investigation combines atomically resolved *in situ* heating in a scanning transmission electron microscope (STEM) and STEM simulations with temperature-programmed x-ray photoelectron spectroscopy (TP-XPS) in the room temperature to 750 °C range. Using these techniques, we follow the surface group coordination at the atomic level. It is concluded that the F and O atoms compete for the DFT-predicted thermodynamically preferred site and that at room temperature that site is mostly occupied by F. At higher temperatures, F desorbs and is replaced by O. Depending on the O/F ratio, the surface bare MXene is exposed as F desorbs, which enables a route for tailored surface functionalization.

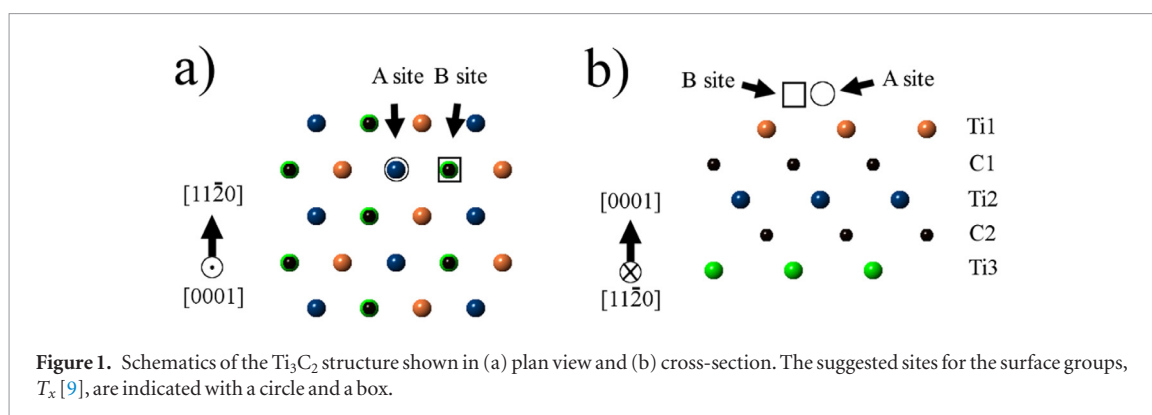
Introduction

Since the discovery of graphene [1], two-dimensional (2D) materials have attracted vast attention as a consequence of their exceptional properties that arise from their reduced dimensionality as compared to their parent bulk materials. A few years ago, a new family of 2D transition metal carbides, MXenes, was discovered [2–4]. MXenes have been described as *2D-conductive clays* [5] synthesized by exfoliation of the MAX phases, which are nanolaminated phases of carbides and/or nitrides following the general formula $\text{M}_{n+1}\text{AX}_n$ ($n = 1, 2$ or 3), where M is an early transition metal, A is a group A element, and X is either C or N [6]. To produce MXene, the MAX phase is chemically etched, resulting in the selective etching of the A layers and their replacement with surface termination. Accordingly, their proper designation is $\text{Ti}_3\text{C}_2\text{T}_x$, where T_x consist of surface termination groups that include O, OH and F [7]. The resulting multilayer particles are weakly bound together and can subsequently be

separated resulting in 2D metallic-like $\text{M}_{n+1}\text{X}_n\text{T}_x$ sheets.

MXene's 2D nature, their good electronic conductivity [5], hydrophilicity in combination with the possibility to terminate their surfaces with various functional groups [2, 3, 8–10] and the ability to intercalate the MXene sheets [11, 12], render them highly attractive for, e.g. energy storage application such as Li-ion batteries [8, 11, 13, 14], and electrochemical capacitors [11, 15, 16]. From the number of MXenes produced to date (>20) in combination with the range of possible coordinations by surface terminating groups, the tailoring potential in this family of materials is noteworthy.

The coordination of the surface terminating groups on the MXene surfaces is predicted to strongly influence the material properties, including energy storage capacity [8], magnetism, band gap energy [9] and surface plasmon resonance [17, 18]. Depending on the chemical etching process, the composition of T_x may vary significantly. However, unambiguous results



on the identification and coordination of these surface-terminating groups have yet not been presented. Therefore, studying the coordination of T_x is a research topic of particular interest and importance. Density functional theory (DFT) calculations predict that of two possible sites for the T_x the A-site is the more energetically favorable [9]. The A-site is defined to be on top of the central Ti atoms, as shown in the plan- and cross-sectional views of the $\text{Ti}_3\text{C}_2\text{T}_x$ structure presented in figures 1(a) and (b), respectively; the A-site in figure 1 is denoted by a circle. Included in figure 1 is also the B-site, which is defined to be on top of the central C atoms denoted in figure 1 by a square.

Among the many MXenes reported to date, $\text{Ti}_3\text{C}_2\text{T}_x$ is by far the most investigated. Herein we use this benchmark MXene to investigate the coordination of the adsorbed surface groups, T_x , together with their thermal behavior during heating up to 750 °C. The investigation is performed by temperature-programmed x-ray photoelectron spectroscopy (TP-XPS) and atomically resolved *in situ* scanning transmission electron microscope (STEM).

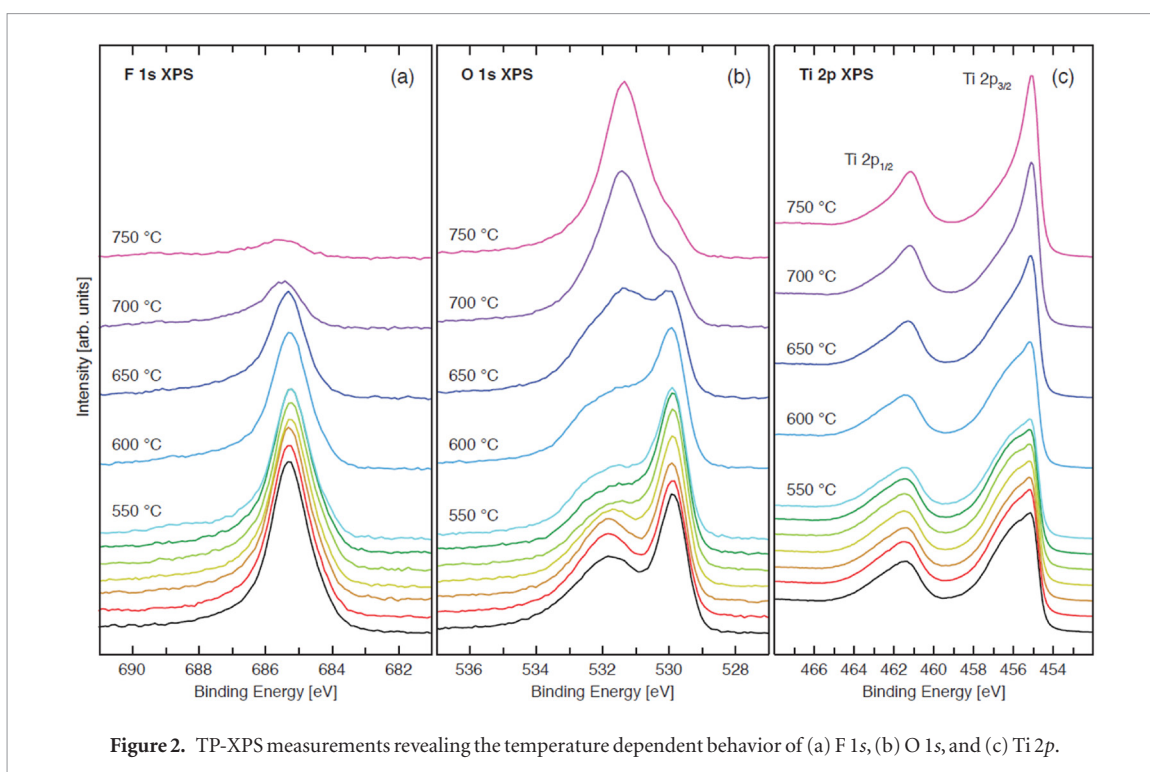
Methods

Thin film $\text{Ti}_3\text{C}_2\text{T}_x$ samples used for the XPS measurements were prepared by first depositing Ti_3AlC_2 on *c*-axis-oriented sapphire, Al_2O_3 , $10 \times 10 \text{ cm}^2$ surface area substrate using DC magnetron sputtering in an ultrahigh vacuum system. The deposition was performed using elemental Ti, Al and C targets with diameters of 75, 50 and 75 mm, respectively. Prior to deposition the substrate was preheated inside the deposition chamber at 780 °C for 1 h. The Ti and C targets were ignited at 780 °C with powers of 92 and 142 W, respectively, for 30 s forming an incubation layer of TiC before the Al target is ignited at a power of 26 W. The duration of sputtering is 10 min, which produces a film about 30 nm thick. Immediately after the Ti_3AlC_2 thin film was removed from the PVD system it was converted into $\text{Ti}_3\text{C}_2\text{T}_x$ by etching in 10% concentrated HF(aq) (Sigma Aldrich, Stockholm, Sweden) for 1 h at RT. After etching, the sample was rinsed in deionized water and ethanol. The etching and washing procedure used here has been demonstrated to result in a small increase in

the lattice parameter because of the incorporation of the surface groups. Furthermore, the thickness of the film stays approximately the same after etching and washing. More details on sample preparation can be found elsewhere [17]. For this study it was important that the exposure to the atmosphere was kept as short as possible. The $\text{Ti}_3\text{C}_2\text{T}_x$ sample was therefore placed in the XPS instrument shortly after the etching process was performed. Impurities, such as TiO_2 and Al_2O_3 , and contamination, such as hydrocarbon and alcohol compounds, could thereby be kept at an insignificant level.

The $\text{Ti}_3\text{C}_2\text{T}_x$ multilayered powder samples used for the STEM experiments were prepared by etching Ti_3AlC_2 powders. The latter were synthesized by mixing commercial Ti_2AlC powders (Kanthal, Sweden, –325 mesh) with TiC (Alfa Aesar, Ward Hill, USA, 99.5 wt.% purity, –325 mesh) in a 1:1 molar ratio (after adjusting for the ~12 wt.% Ti_3AlC_2 already present in the commercial Ti_2AlC powder) followed by ball milling for 18 h to ensure proper mixing. The powders were subsequently heated in a tube furnace to 1350 °C with a rate of 10 °C min^{-1} for 2 h under flowing Ar. The resulting material, in the form of a lightly sintered brick, was ground milled using a TiN-coated milling bit and sieved through a 400 mesh sieve, producing Ti_3AlC_2 powder with a particle size $< 38 \mu\text{m}$. The obtained powders were immersed in 10% HF(aq) in a ratio of 1 mg of Ti_3AlC_2 to 20 ml of solution at RT for 24 h. The resulting suspension was washed with deionized water and separated from the remaining HF(aq) by centrifuging until the pH of the liquid reached a pH between 5 to 6. The separated powders were then finally washed with ethanol and left to dry overnight in air. TEM samples were thereafter prepared by crushing the powder in a mortar with a pestle and dispersing a mixture of the powder and ethanol on a DENSsolutions holey SiN_x Wildfire heater chip and placed in a DENSsolutions double tilt heating holder. Possible particles of Al_2O_3 or other impurities were screened out in the process.

TP-XPS was performed with the AXIS Ultra^{DLD} system from Kratos Analytical Ltd using monochromatic Al $K\alpha$ radiation. The XPS was performed in an analyzer chamber while the temperature-controlled sample heating was performed in an adjoining



preparation chamber; both chambers had a base pressure better than 1×10^{-9} mBar. The sample was heated to a given temperature for 0.5 h. It was then cooled and transferred from the preparation chamber into an adjoining analyzer chamber. After analysis the sample was transferred back to the preparation chamber and the process was repeated with steps of increasing temperatures until the maximum temperature of 750 °C was obtained. Since the sample was supported on an insulating sapphire substrate sample charging was a concern. To avoid inconvenient binding energy shifts caused by sample charging during spectra acquisition, potential depletion of electrons in the sample was compensated by a continuous flow of low energy electrons. The binding energy scale was calibrated against the Fermi-edge (E_f), which was set to a binding energy of 0 eV, and the overall energy resolution was better than 0.5 eV. Normalization of all spectra was performed at the background on the low binding energy side of the main peak/peaks. The TP-XPS was performed in the range of RT up to 750 °C.

The *in situ* heating experiments were performed inside the (S)TEM at temperatures ranging from RT to 750 °C using the same time steps as in the TP-XPS experiment. Characterization was performed using the Linköping double corrected FEI Titan³ 60-300, equipped with a high-brightness gun (XFEG), monochromator, and Quantum ERS-GIF. High-resolution TEM images during *in situ* annealing were acquired at 60 kV. Thickness determination of the MXene sheets was performed through intensity variations in the STEM HAADF images. The high-resolution STEM images were acquired at 300 kV and <10 pA beam current. STEM image simulations (see supplementary information for details) (stacks.iop.org/

[TDM/5/015002/mmedia](http://stacks.iop.org/TDM/5/015002/mmedia)) were performed using the Dr Probe software [19]. STEM image analysis was carried out using built-in routines for the commercially available Digital Micrograph and Matlab (see supplementary information for details).

Results and discussion

The aim of the present study is to provide experimental evidence on the identification and coordination regarding the termination groups on 2D sheets. It is therefore essential that the studied sample is kept as clean as possible, e.g. by reducing the exposure to the atmosphere to minimum duration. Owing to the extra precaution, contamination was found to be at an insignificant level. For example, figure S1 shows that the amounts of hydrocarbons and alcohol compounds are quite small and are estimated to be less than 3%. In addition, the TiO₂ contribution is also too low to be estimated. Comparison with previously presented XPS spectra of Ti₃C₂T_x [7] shows that the thin film Ti₃C₂T_x sample in the present work has significantly less impurities and contamination. Further discussion regarding sample impurities and contamination can be found in the supplementary information.

Figures 2(a)–(c) present, respectively, the F 1s, O 1s, and Ti 2p TP-XPS spectra of a Ti₃C₂T_x thin film on sapphire ranging from room temperature (RT) to 750 °C. As the temperature increases, the F 1s, O 1s, and Ti 2p spectra transform in response to changes in the quantities and coordinations of T_x. Most apparent is the loss in F 1s intensity (figure 2(a)) while the integrated intensity of the O 1s and Ti 2p spectra remain more or less constant throughout the TP-XPS study (see supplementary information figure S2).

The temperature-dependent intensity redistributions of the O 1s and Ti 2p provide valuable information about coordination sites for T_x on the Ti_3C_2 surfaces. The C 1s spectrum (shown in supplementary, figure S1) maintains a stable signal throughout the experiment, indicating that no loss of C occurs. More importantly, the stable C 1s signal at 282.0 eV indicates that the MXene does not undergo any reactions or phase transformations upon heating up to 750 °C.

The F 1s XPS spectrum at RT contains a single sharp peak at 685.3 eV, which indicates the existence of one F containing species that coordinates to a single site. The corresponding O 1s XPS spectrum contains two peaks centered at 529.9 and 531.9 eV, respectively suggesting two distinctly different surface O containing species or one species occupying two different sites. The Ti 2p XPS spectrum at RT shows the two spin-orbit split features $2p_{3/2}$ and $2p_{1/2}$ around 455.9 and 462.0 eV, respectively. A closer inspection suggests that the $2p_{3/2}$ consists of two peaks separated by only about 1 eV indicating at least two different Ti coordinations, which the higher broadening of the $2p_{1/2}$ cannot distinguish. The origin of the two Ti $2p_{3/2}$ peaks, located around 455.1 and 455.9 eV, suggests that the Ti atoms are coordinated with two different termination groups.

Up to 500 °C the $Ti_3C_2T_x$ sample is stable and the only change observed in the F 1s, O 1s, and Ti 2p TP-XPS spectra is the gradual intensity redistribution of the O 1s from 531.9 to 529.9 eV, i.e. from higher to lower binding energy peaks. In the 550–750 °C temperature interval, on the other hand, the F 1s peak intensity reduces to a fraction of its original intensity. Hence, F-species desorb from the Ti_3C_2 surfaces at elevated temperatures. More dramatic changes are also observed in the O 1s spectra where the peak at 529.9 eV is significantly reduced while a third peak grows at 531.3 eV; the latter dominates the O 1s spectrum after the 750 °C heat treatment. A parallel behavior is observed for the Ti 2p peak where the intensity redistribution benefits the growth of the Ti $2p_{3/2}$ peak at 455.1 eV and Ti $2p_{1/2}$ peak at 461.2 eV.

The F 1s spectra in figure 2 shows that the F desorption process is not complete even after the 750 °C heat treatment and the O 1s and Ti 2p spectra therefore still show the 529.9 and 455.9 eV features as shoulders on the main peaks. Nevertheless, the sharp O 1s and Ti $2p_{3/2}$ main peaks at 531.3 and 455.1 eV, respectively, implies that there is only one surface group that prevails after a thorough high-temperature heat treatment in vacuum. In addition, the fact that the reduction in the F 1s intensity coincides with the decrease in the Ti $2p_{3/2}$ intensity around 455.9 eV suggests that the high binding energy Ti $2p_{3/2}$ feature originates from Ti with adsorbed F, which implies that the Ti $2p_{3/2}$ peak at 455.1 eV originates from Ti with adsorbed O species, as is expected from the HF(aq) etching [2, 3], and possibly uncoordinated Ti. However, the sharp Ti $2p_{3/2}$ and O 1s peaks at 455.1 and 531.3 eV, respectively, indicate that after the heat treatment at 750 °C, i.e. after most of

the F has desorbed, the O containing species can only be either O or OH. That means that if both O and OH are present as surface terminating groups in the etching process, then one of them must desorb or transform into the other during the heat treatment. It is feasible that the broad Ti $2p_{3/2}$ peak at RT could consist of three features, although any proposed third peak must: (i) be stable up to but, (ii) start to reduce in intensity at the same temperature as the F starts to desorb. More information can, on the other hand, be gained from the O 1s spectrum. The integrated intensity for the O 1s spectra does not change significantly during the study, from which one can infer that no O-containing species has desorbed from the Ti_3C_2 surface. (The integrated intensity for F 1s, O 1s, Ti 2p, and C 1s spectra of $Ti_3C_2T_x$ ranging from RT to 750 °C is shown in supplementary information figure S2.)

Moreover, the absence of an integrated intensity reduction of the O 1s TP-XPS spectra implies that an OH dissociation has not occurred, because were that the case the dissociation product H would react with neighboring OH and form H_2O that would desorb immediately at temperatures above 500 °C and decrease the integrated intensity of the O 1s spectra accordingly. Hence, a significant transformation from OH into O can be excluded. In addition, a transformation from O into OH can also be removed from consideration because that would require a substantial amount of hydrogen supplied to the Ti_3C_2 surface. Consequently, there can only be one O containing species introduced at the etching process and that species stays intact throughout the heat treatment up to 750 °C. The instability of OH on Ti surfaces at higher temperatures [20] (O 1s integrated intensity is expected to diminish), the fact that surface OH is prone to react and form water that would later desorb (reducing the O 1s signal), and that OH is in general not very mobile (O 1s signal should exhibit no peak shifts in the TP-XPS) are three contradictions to what we observe in our XPS data. This leads us to conclude that little or no OH is present on the $Ti_3C_2T_x$ surface. Altogether, the information gained from the TP-XPS study indicates that the single O containing species is atomic oxygen that is mobile on the Ti_3C_2 surface, can occupy two adsorption sites on the Ti_3C_2 surface, and is stable at temperatures up to 750 °C.

The peak positions and intensity redistribution observed in the TP-XPS study implies that the F is adsorbed on one specific and well-defined site on the Ti_3C_2 surface and that O is adsorbed on two different sites where one is the same preferred adsorption site as for the adsorbed F. It is proposed that during the HF(aq) etching of Ti_3AlC_2 the F and O atoms compete over the same preferred site on the Ti_3C_2 surface. While F occupies only one adsorption site, O resides on two alternative sites. The O 1s intensity redistribution in the temperature interval of 300–500 °C suggests that O on the preferred absorption site moves to the alternative site because of influences from F, i.e. charge

transfer from Ti to the adsorbed F makes the preferred site less attractive for the adsorbed O. Said otherwise, Ti_3C_2 surface favors adsorbed F on this specific site and the less favored O is relegated to the alternative site. However, when F desorbs, at temperatures above 550°C , the preferred site becomes available and a complete redistribution follows when O rearranges from the alternative site to the preferred.

The intensity redistribution of the Ti $2p$ peaks reveals a charge transfer from the adsorbed F back to Ti_3C_2 prior to F desorption (the shoulder at 455.9 eV diminishes while the intensity at 455.1 eV increases after F desorption). With the highest electronegativity of all elements, F attracts significantly more electrons from the Ti_3C_2 as compared to O. The consequence is an uneven charge distribution with reduced electron density on the Ti atoms coordinated to F compared with Ti atoms that are not. The local electron density valleys, which are positive with respect to the surroundings, will attract delocalized electrons in order to screen it, which causes a strengthening of the covalent Ti–C bonds in Ti_3C_2 [21, 22]. This charge transfer from the Ti atoms to the adsorbed F, and consequently the distribution of the delocalized electrons, presumably causes a relatively reduced charge transfer to the O adsorbed on the preferred site when O is co-adsorbed with F compared to the charge transfer to the adsorbed O from the Ti_3C_2 surface after the F has been desorbed. This is proposed here as the reason why the high binding energy peak in the O $1s$ spectra shifts -0.4 eV when the situation for O on the Ti_3C_2 surface changes from being co-adsorbed with F to being the sole terminating group.

The TP-XPS shows that there is a preferred absorption site for the F and O atoms and that O also (while F is in the preferred site) occupies an alternative site. The observations that (i) the Ti $2p$ peaks go through a significant intensity redistribution upon desorption of F, (ii) the C $1s$ peak do not show any significant binding energy shifts (figure S1), and (iii) the origin of the high binding energy peak in the O $1s$ spectrum is the preferred site, and that the two O $1s$ peaks are separated by $\sim 1.5\text{ eV}$, suggests that the preferred absorption site for both F and O might be, e.g. a hollow site and the alternative O site, e.g. a bridge site [23]. To confirm this, a corresponding high-temperature investigation was performed inside the (S)TEM.

Figure 3 shows sequential TEM images from a corner of a MXene multilayer particle as a function of increasing temperatures (see Methods for details on synthesis). At ambient temperature, disorder is strongly visible in addition to the ordered structure of the MXene sheets, see figure 3(a). The disordered material is interpreted as a mixture of C-based molecules that originate from the TEM sample preparation procedure and adsorbed functional groups originating from the $\text{HF}(\text{aq})$ etching process. The majority of the C-based molecules are removed at temperatures slightly above 100°C . Hence, the 300°C

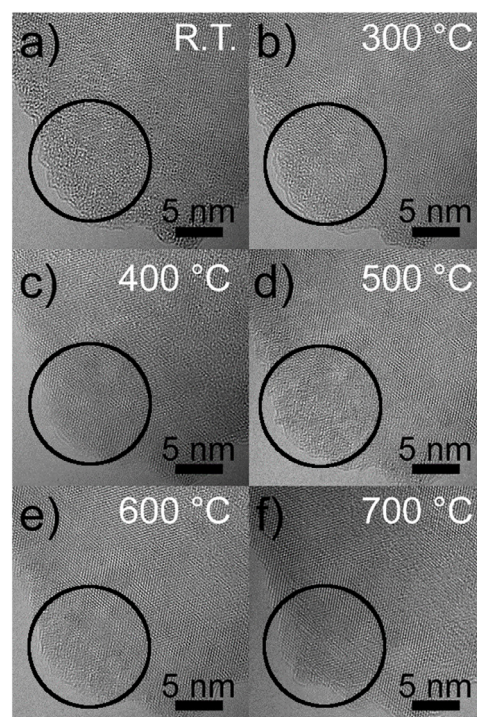


Figure 3. Temperature dependent low-kV (60 kV) TEM images of a multilayered MXene particle. (a), (b), (c), (d), (e), and (f) are acquired at RT, 300°C , 400°C , 500°C , 600°C and 700°C respectively. Increased order at elevated temperatures is observed at the edge of the particle (circles).

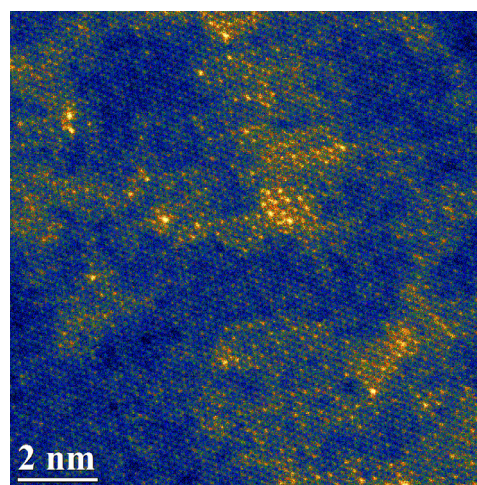


Figure 4. False color atomically-resolved plan-view STEM image of a single $\text{Ti}_3\text{C}_2\text{T}_x$ sheet acquired at 500°C after previous heating to 700°C for 30 min.

image in figure 3(b) appears slightly cleaner, although disorder is still present. The images at 400 and 500°C in figures 3(c), (d) show a similar appearance, marginally improving with temperature. However, at 600°C and in particular at 700°C , the image indicates that the particle appearance is significantly affected by the applied heating. Most notable is the improvement in the thinnest regions and at the edges (interfacing vacuum), that assume a distinctly faceted outline. Additionally, the image now visibly demonstrates Fresnel

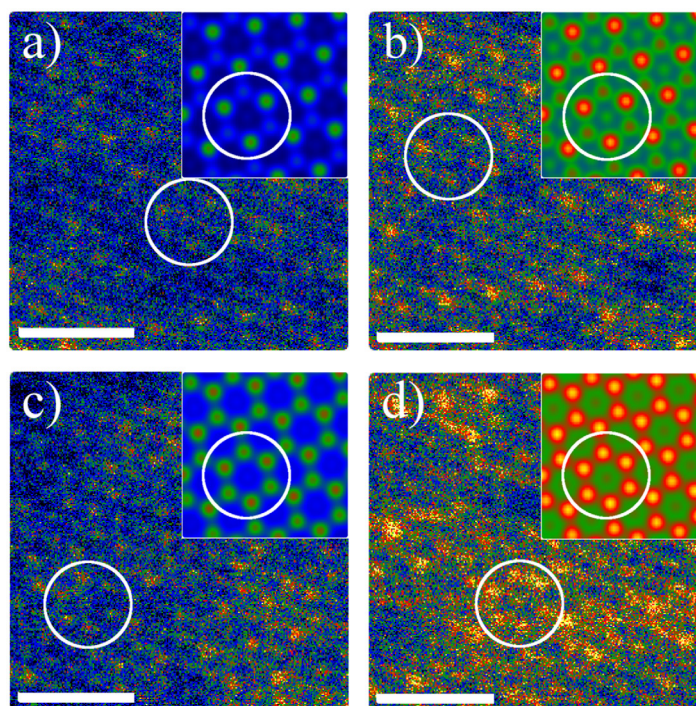


Figure 5. False color STEM intensity patterns of enlarged selections from figure 4. (a) Bare Ti_3C_2 surface (b) O adatoms occupying A-sites on the bottom MXene surface (c) O adatoms on A-sites on top surface, and (d) O adatoms occupying A-sites on both top and bottom surfaces. Insets show correlated STEM simulation of respective surfaces. (Scale bar 0.5 nm.)

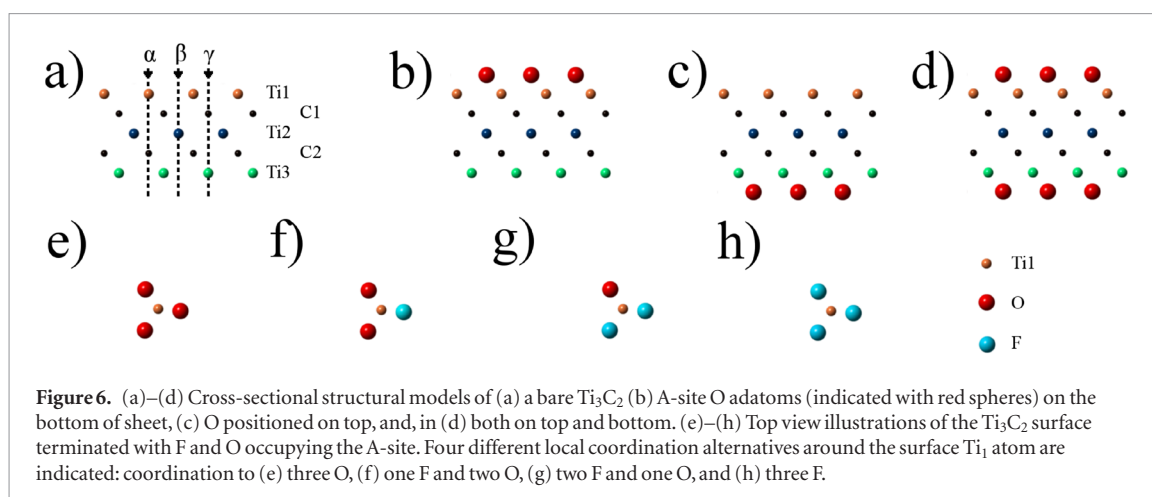
contrast based dark lines that outline the surface steps, between the various MXene layers, which run alongside the outline of the particle. Most importantly, the structure has assumed a significantly crisper appearance and the initial disorder is lost.

Fast Fourier transformations (not shown) of the images indicate that the MXene structure itself has not undergone any phase changes, which can also be understood from the preservation of the microstructural features. It is recalled that TP-XPS showed no loss of Ti, C or O although a significant reduction of F from the Ti_3C_2 surface was observed. Consequently, the observed changes through the image series are attributed to the reduction of F and the reorganization of O atoms.

To investigate the organization further, and to identify the atomic structure of the heat-treated MXene, high-resolution STEM imaging was performed on a single sheet at elevated temperatures. The plan-view image that is shown in figure 4 was acquired at 500 °C, after pre-heating up to 700 °C for 30 min (instabilities at temperatures >500 °C caused difficulties in acquiring high-resolution images). The image reveals patches of different intensities and symmetries. A closer inspection of these areas further identifies different surface patterns as exemplified in figures 5(a)–(d). Intensity normalization was performed on the tails extending into vacuum; more details are given in the supplementary material. The least intense areas shown in figure 5(a), exhibit a weakly increased intensity at every third projected atom column and forms a more sparsely occupied close packed structure compared to the MXene as exemplified in figure 5(c) (peak intensity positions

exhibit a red color, while background peak positions are blue–green). In figure 5(b) the pattern is similar, although the average intensity is higher with peak intensity columns in the red–yellow range. The pattern in figure 5(c), with a slightly increased background intensity compared to that in figure 5(a), exhibits high intensity atomic columns organized in a honeycomb-like pattern. These columns additionally surround a slightly less intense column. Through close inspection it is revealed that every second atomic position of the honeycomb hexagon exhibits a faintly elevated intensity over the neighboring high intensity positions. The background intensity additionally varies in the image, e.g. the honeycomb structure centered in the image exhibits a higher intensity compared to the adjacent honeycomb at the bottom right. Finally, the image in figure 5(d) exhibits brighter features that also form a honeycomb-like structure, similar to figure 5(c), on an additionally increased intensity background.

In order to interpret these different patterns, we simulated various STEM images as a function of surface termination and their distributions and the results are shown as insets in figure 5 (additional simulations are shown in the supplementary material). The structures considered for the simulated insets are shown in figure 6. This includes; (a) a single bare (T_x -free) Ti_3C_2 MXene sheet, (b) O coverage on the bottom of a Ti_3C_2 sheet (i.e. on the exit wave surface), (c) O on top (i.e. facing the electron beam) and, (d) O coverage on both surfaces. The proposed O site (A-site, see figure 1) stems from previous work where x-ray and neutron scattering atomic pair distribution func-



tion experiments were used to determining the bond lengths of Ti–C/O/F in $\text{Ti}_3\text{C}_2\text{T}_x$ MXenes [24, 25]. Other possible sites for O were additionally considered but were ruled out after comparison to the experimental images and for symmetry reasons (O should choose equivalent positions on both surfaces). The surface models were matched quantitatively by comparing atomic column intensity levels and additionally by intensity pattern distributions of neighboring columns. For a more detailed discussion see supplementary material (figures S11 and S12). Notably, the atomic column intensity does not reflect the commonly generalized Z^2 scattered intensity for atomically resolved STEM images [26]. This is particularly visible for the bare MXene. By comparing to the structure model applied in this simulation (inset in figure 5(a)), the projected column that includes Ti_1 and C_1 atoms (column α in figure 6(a)) returns the highest intensity and forms a sparse close packed appearance. In contrast, the projected column containing C_2 and Ti_3 atoms (column γ in figure 6(a)) returns the lowest intensity. The Ti_2 layer (projected column β in figure 6(a)) returns an intermediate intensity. The mechanism behind the different contrast is further discussed in the supplementary material. Astonishingly, the simulated images indicate that it is possible to identify the top and bottom surfaces of the sheet, simply through intensity variations. Comparing the simulated bare MXene in figure 5(a) with the low intensity regions represented in the experimental image the structure matches qualitatively, which, indicates that these low intensity regions constitute bare Ti_3C_2 areas. In air and at ambient conditions, this state would be remarkable; it is less so in the ultrahigh vacuum environment of the TEM after heating to 750 °C.

The simulated image in figure 5(b) comprise a single sheet MXene covered with O adatoms on the A-sites (figure 6(b)) on the bottom surface. In analogy with the intensity of the exit surface Ti_3 atoms, the lower mass of bottom surface O adatoms add little contrast to the simulated image individually. However, the background intensity of the simulated image has increased, raising the intensity of all atomic columns.

Again, the most intense columns correspond to those that include the Ti_1 atoms, and the results compare well with the observed background intensity increase observed in figure 5(b).

In figure 5(c) the O adatoms reside on the A-site on the top surface. As can be observed from the simulated image, the additional O adatoms, result in columns that form a honeycomb-like pattern with a lower intensity column in the center. The atomic columns of the honeycomb hexagon exhibit similar, although slightly different, projected intensities with the column exhibiting the Ti_1 atom returning a slightly higher intensity.

Figure 5(d) shows the results from a simulation exhibiting O adatoms on A positions on both surfaces. The honeycomb pattern is preserved, however the background intensity is further elevated and the highest intensity columns here correspond to columns containing the O adatom on the top surface. The simulation results as shown in the insets in figures 5(c) and (d), indicate that the varying intensity of the honeycomb pattern observed in figure 5(c) is the result of partial O coverage on both surfaces.

The honeycomb patterns observed across figure 4, hence serve as distinct fingerprints of the preferred O position after high-temperature heating. Simulations for other configurations were performed but failed to return the honeycomb pattern (figures S7(d) and (e)). Consequently, this indisputably verifies the A-site as the preferred position for the O adatom in total accord with the XPS results.

Locally, figure 4 additionally displays even brighter atomic positions. These positions are after simulation (supplementary information figure S6) interpreted as Ti adatoms. The darkest intensities in the sheet are interpreted as Ti vacancies. Statistical analysis further supports this interpretation by the observed approximately 1:1 ratio of darkest lattice positions and brightest lattice positions (Ti vacancies and Ti adatoms).

The identification and favored position of the surface groups T_x is essential information for a comprehensive understanding and control of MXene properties, such as charge capacity and ion mobility

for, e.g. electrochemical applications. Until now, a number of papers have been published reporting on the theoretical prediction of preferred sites for different functional groups [27, 28]. In this work we reveal, for the first time, the preferred positions of the O and F surface adatoms by employing a combined temperature-programmed XPS and direct observation high-resolution (S)TEM imaging of $\text{Ti}_3\text{C}_2\text{T}_x$. It is found that the F terminations only occupy A-sites and that the O atom preferably occupies the same site although F takes precedence over O. Thus, while the F atoms occupy the preferred site, the O also resides on an alternative site, which presumably causes the apparent disorder observed prior to heating (figure 3(a)). This alternative site remains unidentified though it is proposed to be a bridge site. It has been observed that O surface adatoms are highly mobile on Ti_3C_2 surfaces even at ambient temperatures [29]. This may indicate that the alternative site exhibits a low binding energy, as discussed in the results, contributing to the observed disorder. In contrast, the surface configuration after heating to 750 °C is highly stable, even at the 500 °C elevated temperature used during image acquisition, shown in figure 4.

In a previous XPS work [7], peaks between 531.2 eV and 532.0 eV were assigned to C–Ti–O_x, C–Ti–OH_x, bridging OH groups on TiO_2 , and/or organic compounds. Based on the present work all these peaks can be assigned to atomic O sitting on the thermodynamically preferred A-site with small variations in the local bond configuration. Furthermore, based on the results shown herein and in total agreement with the finding that at the highest temperatures the O occupies the A-sites, we can more confidently propose the peak at 529.9 eV to atomic O bridging two Ti sites on the MXene surface and not a TiO_2 surface. This finding contradicts the majority of reports in the field, which consider OH termination to be the more likely functional group. However, in agreement with the present work, a recent NMR investigation identifies O to be the dominant functionalizing element on Ti_3C_2 surfaces [30].

With the HAADF-STEM identification of preferred terminations in mind, it is motivated to perform curve fitting of the XPS spectra, as shown in figure S1(b). The curve fitting of the F 1s spectra requires two curves at 684.5 and 685.3 eV to fit the slight asymmetry of the spectrum profile. The former is suggested to represent F occupying the A-site without influences from other adsorbates while the latter, the main component of F 1s, represent influences from co-adsorbed O. The O 1s spectra are curved fitted with two or three curves. The curves at 529.9 and 531.9 eV originate from adsorbed O at the alternative site and at the preferred A-site, respectively. The high binding energy curve is relatively broad, which indicates different local environment of the probed O atoms on the A-site. This is a consequence of the highly mobile O on the Ti_3C_2 surface [29] and that O is co-adsorbed with F in different local bond configurations. However, at

temperatures above 600 °C a third curve at 531.3 eV is required. This curve represents O on A-sites that are not influenced by co-adsorbed F. The Ti 2p spectra are curved fitted with three pairs of curves. The three curves that represent the Ti 2p_{3/2} are at 455.1, 455.9, and 456.9 eV and the corresponding curves for the Ti 2p_{1/2} are at 461.2, 462.0, and 463.0 eV. The pair of curves at 455.1 and 461.2 eV originates from Ti with a local adsorption of only O, while the pair of curves at 456.9 and 463.0 eV originates from Ti with a local adsorption of only F. The pair of curves at 455.9 and 462.0 eV originate from Ti with a local environment that is influenced from both F and O.

The curve fitting of the Ti 2p XPS can be illustrated as shown in figures 6(e)–(h). These figures identify O or F adatoms on A-sites surrounding a Ti1 atom (in this top-view projection). Each surface Ti₁ is surrounded by a combination of three F and O atoms: O–O–O (denoted $\text{Ti}_3\text{C}_2\text{T}_\text{O}$), O–F–O and F–O–F (denoted $\text{Ti}_3\text{C}_2\text{T}_\text{F,O}$), and F–F–F (denoted $\text{Ti}_3\text{C}_2\text{T}_\text{F}$). Hence, Ti atoms can be affected by only O, only F, or both F and O. The asym-GL curve that fits the Ti 2p_{3/2} peak at 455.1 eV originates from $\text{Ti}_3\text{C}_2\text{T}_\text{O}$. The other curves are related to Ti atoms that are affected by the adsorbed F occupying the A-site as in figures 6(f)–(h). When Ti atoms are affected by both F and O, the Ti 2p_{3/2} is shifted by 0.8 eV and when Ti atoms are affected by only F (figure 6(h)) the Ti 2p_{3/2} is shifted further to 456.9 eV. These chemical shifts can be explained by the higher electronegativity of F compared to O which attracts significantly more electrons from the Ti_3C_2 sheet. Potentially, small chemical shifts also exist between Ti atoms with F–O–F and O–F–O configurations that would require additional curves for a more accurate curve fitting of the Ti 2p_{3/2}. Even further combinations are possible if the influences from the O atoms on the alternative site are included or if there are vacancies in the F and O adsorbate structures. Nevertheless, details of the F and O combinations on the A-sites and the influences from the O adsorbed on the alternative site are not obtained in this work, although the two curves representing $\text{Ti}_3\text{C}_2\text{T}_\text{F,O}$ and $\text{Ti}_3\text{C}_2\text{T}_\text{F}$ have relatively larger FWHM, compared to the curve representing $\text{Ti}_3\text{C}_2\text{T}_\text{O}$, suggesting that the F related Ti 2p_{3/2} feature around 455.9 eV could very well consist of more than two components, separated by only a few tenths of an eV.

The obtained parameters from the curve fitting of the F 1s, O 1s, and Ti 2p XPS spectra are summarized in table 1. Included are also the obtained parameters from the curve fitting of the C 1s XPS spectra (see figure S1(a)).

This investigation also reveals that a high-temperature heating process can be utilized to rid the MXene surfaces from F, and to organize available O onto the A-sites. These results suggest that a chemical etching process that functionalizes the MXene surfaces by a high amount of F adatoms can be used together with a subsequent high-temperature heating to produce

Table 1. Parameters obtained for the curve fitting of F 1s, O 1s, and Ti 2p of $Ti_3C_2T_x$.

Element	Component	1s (eV) ^a	2p _{3/2} (2p _{1/2}) (eV) ^a	FWHM (eV) ^b
F 1s	Ti–C–T _F	684.5		1.0
	Ti–C–T _{FO}	685.4		1.0
O 1s	Ti–C–T _O (2nd site)	529.9		0.89
	Ti–C–T _O (A-site)	531.3		1.2
	Ti–C–T _{FO} (A-site)	531.9		1.6–2.3 ^c
Ti 2p	Ti–C–T _O		455.1 (461.2)	0.70 (1.4)
	Ti–C–T _{FO}		455.9 (462.0)	1.1 (1.9)
	Ti–C–T _F		456.9 (463.0)	1.1 (1.9)
C 1s	Ti–C–T _x	282.0		0.64
	C–C	284.3		1.3
	CH _x	285.2		1.3
	C–OH	286.4		1.3

^a The binding energies are determined within ± 0.1 eV.

^b Full width at half maximum (FWHM) for the Gaussian–Lorentzian curves.

^c The FWHM for the curve representing O at the A-site at the temperatures interval of 200–600 °C increased from 1.6 to 2.3 eV.

predominantly bare and un-functionalized MXene. An opposite etching process, which results in reduced F adatom surface coverage, could be applied to obtain highly ordered and predominantly O functionalized surfaces after heating. The properties of these exemplified MXenes are beyond the scope of this work and are left to the community to address. Lastly, the stability of these emerging structures as these 2D flakes are exposed to ambient conditions remains to be investigated.

Conclusions

In conclusion, the organization of surface groups on $Ti_3C_2T_x$ MXene was investigated as a function of temperature. Through temperature-programmed XPS it was shown that the functional groups consist of F and O occupying well-defined sites on the Ti_3C_2 surfaces. While the functional F coordinates to a single site, the functional O coordinates to two sites. As the temperature exceeds 550 °C, the functional F gradually desorbs and is essentially removed at 750 °C. Upon F desorption the O surface atoms that coordinates to the alternative site, which most likely is a bridge position, migrate to the preferred coordination vacated by the desorbed F.

In situ heating of a few layers of $Ti_3C_2T_x$ sheets in the TEM shows that the initial surface disorder transforms into highly ordered structures at temperatures corresponding to the reconfiguration temperatures observed by the TP-XPS. In addition, through high-resolution STEM imaging and corroborating STEM image simulations the functional O atoms were found

to thermodynamically favor the A-sites, i.e. on top of the Ti atoms of the middle layer. Hence, the MXene heating process is suggested to be vital for further research efforts as it enables surfaces with well defined coordinations. It also leaves part of the MXene surface bare and unfunctionalized, such that further functionalization can be introduced. The heating process may thus serve as a route towards manipulating the functionalization of MXene surfaces. Together, these findings would prove valuable towards improved performance for MXene materials in, e.g. supercapacitor and battery applications.

Acknowledgments

The authors acknowledge the Swedish Research Council for funding under grants no. 621-2012-4359, 622-2008-405, 2013-5580, 2016-04412, 642-2013-8020, and the Knut and Alice Wallenberg's Foundation for support of the electron microscopy laboratory in Linköping, for project funding (KAW 2015.0043), and a Fellowship program. The authors also acknowledge Swedish Foundation for Strategic Research (SSF) through the Synergy Grant FUNCASE, Future Research Leader program and the Research Infrastructure Fellow program (RIF14-0074). The authors additionally acknowledge support from the Swedish Government Strategic Research Area in Materials Science on Functional Materials at Linköping University (Faculty Grant SFO-Mat-LiU No 2009 00971).

Supporting information

Detailed experimental procedures, XPS data and curve fitting, TEM images, and interpretation are presented. (PDF).

Author contributions

J H carried out the growth. L-Å N performed the XPS experiments and analysis. I P, J P, P O Å P performed the TEM/STEM experiments. I P conducted the STEM simulations. I P, J P, P O Å P performed the TEM/STEM analysis. I P, L-Å N, P O Å P prepared the manuscript. All authors assisted in finalizing the manuscript. M W B, V D, J R, J P, P O Å P supervised the work.

Notes

The authors declare no competing financial interest.

ORCID iDs

Per O Å Persson  <https://orcid.org/0000-0001-9140-6724>

References

- [1] Novoselov K S, Fal'ko V I, Colombo L, Gellert P R, Schwab M G and Kim K 2012 *Nature* **490** 192
- [2] Naguib M, Kurtoglu M, Presser V, Lu J, Niu J, Heon M, Hultman L, Gogotsi Y and Barsoum M W 2011 *Adv. Mater.* **23** 4248
- [3] Naguib M, Mashtalir O, Carle J, Presser V, Lu J, Hultman L, Gogotsi Y and Barsoum M W 2012 *ACS Nano* **6** 1322
- [4] Naguib M, Mochalin V N, Barsoum M W and Gogotsi Y 2014 *Adv. Mater.* **26** 992
- [5] Ghidui M, Lukatskaya M R, Zhao M Q, Gogotsi Y and Barsoum M W 2014 *Nature* **516** 78
- [6] Barsoum M W 2013 *MAX Phases: Properties of Machinable Ternary Carbides and Nitrides* (New York: Wiley)
- [7] Halim J, Cook K M, Naguib M, Eklund P, Gogotsi Y, Rosen J and Barsoum M W 2016 *Appl. Surf. Sci.* **362** 406
- [8] Xie Y, Naguib M, Mochalin V N, Barsoum M W, Gogotsi Y, Yu X, Nam K-W, Yang X-Q, Kolesnikov A I and Kent P R C 2014 *J. Am. Chem. Soc.* **136** 6385
- [9] Khazaei M, Arai M, Sasaki T, Chung C-Y, Venkataramanan N S, Estili M, Sakka Y and Kawazoe Y 2013 *Adv. Funct. Mater.* **23** 2185
- [10] Enyashin A N and Ivanovskii A L 2013 *J. Phys. Chem. C* **117** 13637
- [11] Mashtalir O, Naguib M, Mochalin V N, Dall' Agnese Y, Heon M, Barsoum M W and Gogotsi Y 2013 *Nat. Commun.* **4** 1716
- [12] Lukatskaya M R, Mashtalir O, Ren C E, Dall' Agnese Y, Rozier P, Taberna P L, Naguib M, Simon P, Barsoum M W and Gogotsi Y 2013 *Science* **341** 1502
- [13] Naguib M, Come J, Dyatkin B, Presser V, Taberna P-L, Simon P, Barsoum M W and Gogotsi Y 2012 *Electrochem. Commun.* **16** 61
- [14] Eames C and Islam M S 2014 *J. Am. Chem. Soc.* **136** 16270
- [15] Dall' Agnese Y, Lukatskaya M R, Cook K M, Taberna P-L, Gogotsi Y and Simon P 2014 *Electrochem. Commun.* **48** 118
- [16] Rakhi R B, Ahmed B, Hedhili M N, Anjum D H and Alshareef H N 2015 *Chem. Mater.* **27** 5314
- [17] Halim J et al 2014 *Chem. Mater.* **26** 2374
- [18] Mauchamp V, Bugnet M, Bellido E P, Botton G A, Moreau P, Magne D, Naguib M, Cabioch T and Barsoum M W 2014 *Phys. Rev. B* **89** 235428
- [19] Barthe I J 2016 Dr. Probe-STEM simulation software (www.er-c.org/barthel/drprobe/)
- [20] Lu G, Bernasek S L and Schwartz J 2000 *Surf. Sci.* **458** 80
- [21] Hugosson H W, Korzhavyi P, Jansson U, Johansson B and Eriksson O 2001 *Phys. Rev. B* **63** 165116
- [22] Guemmaz M, Mosser A and Parlebas J-C 2000 *J. Electron Spectrosc. Relat. Phenom.* **107** 91
- [23] Björneholm O, Nilsson A, Tillborg H, Bennich P, Sandell A, Hernäs B, Puglia C and Mårtensson N 1994 *Surf. Sci.* **315** L983
- [24] Shi C, Beidaghi M, Naguib M, Mashtalir O, Gogotsi Y and Billinge S J L 2014 *Phys. Rev. Lett.* **112** 125501
- [25] Wang H-W, Naguib M, Page K, Wesolowski D J and Gogotsi Y 2016 *Chem. Mater.* **28** 349
- [26] Crewe A V, Wall J and Langmore J 1970 *Science* **168** 1338
- [27] Gan L Y, Huang D and Schwingenschlögl U J 2013 *Mater. Chem. A* **1** 13672
- [28] Tang Q, Zhou Z and Shen P J 2012 *Am. Chem. Soc.* **134** 16909
- [29] Karlsson L H, Birch J, Halim J, Barsoum M W and Persson P O Å 2015 *Nano Lett.* **15** 4955
- [30] Hope M A, Forse A C, Griffith K J, Lukatskaya M R, Ghidui M, Gogotsi Y and Grey C P 2016 *Phys. Chem. Chem. Phys.* **18** 5099